ANALYSIS OF SOUND SOURCES ON WIND TURBINE BLADES WITH BEAMFORMING AND CLEANT

Marie Hochkirch[1], Timo Schumacher[1] and Henri Siller[1]
[1]German Aerospace Center (DLR), Institute of Propulsion Technology, Department of Engine Acoustics
Müller-Breslau-Str. 8, 10623 Berlin, Germany

Abstract

DLR has developed and built a mobile microphone array for outdoor measurements. First measurements with the new system have been performed in the DLR research wind park WiValdi in Krummendeich. Array data have been measured for different modes of operation of the wind turbines. This paper describes the source localization analysis of the data. The array is mounted on a wooden platform at ground level and has the shape of a multi-arm spiral that has been stretched into an elliptical shape in the direction of the wind turbine in order to improve the resolution in the vertical direction. The geometry of the set-up is not perfect, because the array is not at a right angle to the rotor plane, which moves with the wind direction. Measurements have been performed over 60 seconds. The analysis is performed over a time period covering 5 full rotations, which amounts to a time interval of about 22 seconds.

1 INTRODUCTION

Wind turbines rotate at a near-constant speed. This relatively slow movement generates large-scale turbulences that result in audible pressure fluctuations. These can be recorded using a microphone array and subsequently analyzed. The German Aerospace Center (DLR) designed a microphone array for source localization measurements on wind turbines. The setup of this microphone array is described in [9], which has been presented at DAGA 2026. This paper describes the analysis of the data obtained from that measurement. The aim is to separate sound sources at the three rotor blades and sources at the leading and trailing edges of the blades. Different methods are used to achieve conclusive results while keeping computation costs low.

Figure 1: Wind turbine at the DLR research wind farm WiValdi.

2 METHODS

In order to analyze the wind turbines at the DLR research wind farm WiValdi [4] three different methods were used to evaluate the data obtained from the microphone array. Delay-and-Sum Beamforming is a robust method that gives a good overview of the results. Since the accuracy of this method depends on the imaging poperties of the array that are described by the point spread function, two other methods, CLEANT and CLEANT with grid refinement, were implemented to get better results. All methods are based on classical beamforming.

Since computing time is proportional to the number of points evaluated and the CLEANT algorithm only uses one maximal point in each iteration, the algorithm can be more cost effective by reducing the number of points calculated while looking for the maximum.

2.1 Beamforming

Beamforming uses different sound propagation times and changes in amplitude to reconstruct emitted signals, since both vary with the distance from a source to different microphone positions. By scanning several points on a grid, the source positions can be determined. It is a well known algorithm to reconstruct sound sources and was already established in 1976 by J. Billingsley and R. Kinns [2]. To ensure that sources are reconstructed and localized correctly, the source plane is sampled using an equidistant grid, as shown in Figure 2. Sound sources are expected along the rotor blades. In order to separate sound sources at the leading and trailing edges of the blades, the grid is rotated to be stationary with respect to the rotor plane. As the blade chords taper towards the tip, the grid resolution should be sufficiently dense in this region, where sources are expected.

2.2 CLEANT

The CLEANT algorithm [3] is an extension of the beamforming algorithm, as it reuses its result to find a dominant source in each iteration. The algorithm starts out with classical beamforming. The results are stored as the *Dirty Map*. A *Clean Map* without any data is initialised. From the *Dirty Map* the strongest source in a given frequency domain is identified and its position determined. The source signal is scaled by a loop gain factor $\gamma \in (0,1)$ and added to the *Clean Map*. Since the position is known the microphone signal of the source can be modelled and removed from the total microphone signals, scaled with the same γ. The next iteration uses the

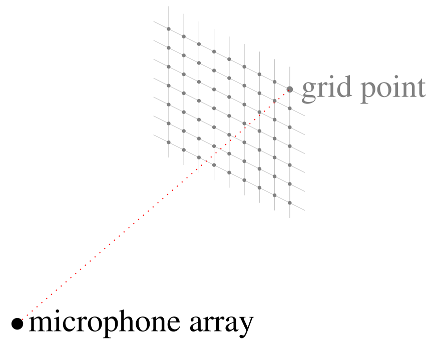

Figure 2: The plane in which the sound sources are expected to be located is defined by a grid, and the grid points are provided to the algorithm as input. The grid points are scanned one by one, thereby locating the sound sources.

reduced microphone signals to again perform beamforming. This process is repeated until the identified point sources reconstruct the recorded microphone data with sufficient accuracy and a stopping criterion is reached [5].

In order for distributed sources along the edge of a rotor blade to be represented accurately in the results, a low scaling factor γ should be chosen as shown in [7]. An example showing results with different values for γ based on a simulated source is displayed in Figure 3.

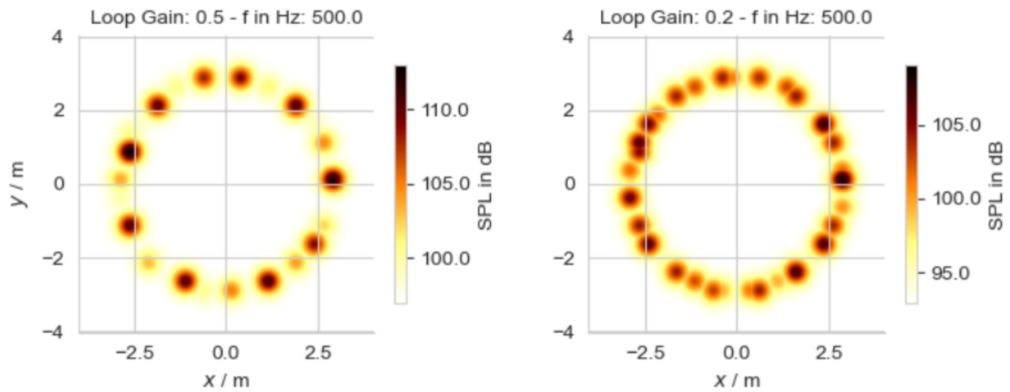

Figure 3: Comparison of CLEANT results with two different values for γ for a simulated ring-shaped source. A lower value for γ results in a better representation of the distributed source. Source: [7]

CLEANT produces a source map that only considers the strongest soures. Iterations continue until the energy in the remaining microphone signals no longer decreases significantly. A flowchart of the algorithm is shown in Figure 4.

2.3 Successive grid refinement

The runtime of the beamforming algorithm is proportional to the number of grid points. Since in each iteration of the CLEANT algorithm, beamforming is performed on a dense grid for high resolution, runtimes are high. As only one source is relevant at each step of the algorithm, it is

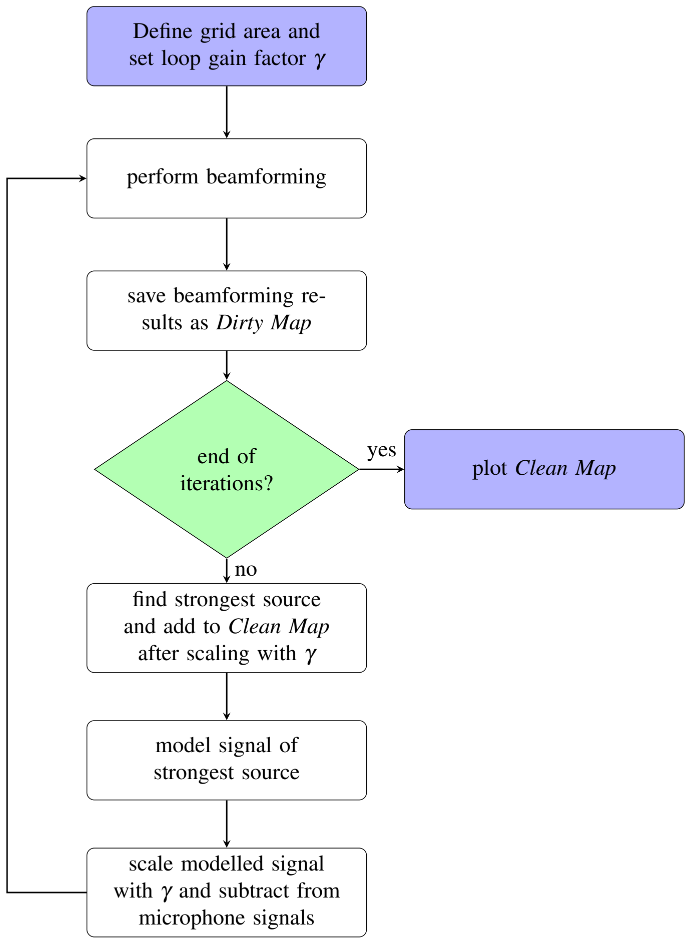

Figure 4: Flowchart of the CLEANT algorithm.

possible to reduce the number of grid points. The idea behind the successive grid refinement method is to scan the source region using a coarse grid and to reduce point spacing only in those areas that contain sources with high sound pressure levels [7]. In order to minimize the risk of undersampling, the point spacing of the initial grid should be smaller than the beam width of the microphone array. This determines the range over which sound sources can be localized and depends on the wavelength of the frequency, the distance between source and microphone array, and the diameter of the array [8]

$$b \sim \frac{\lambda r}{D}. \tag{1}$$

On the initial grid beamforming is performed and a given number of points with maximal values determined in a certain frequency domain. These points are each replaced by four points spaced at half the previous distance. Beamforming is performed on the new points, and again, a given number of points with maximal values is determined. The process continues until a minimal distance between points is reached. This results in quiet regions being largely excluded from the analysis, significantly reducing the processing time. However, as the regions of interest are examined in high resolution, the quality of the results is expected to be similar to that of an equidistant grid.

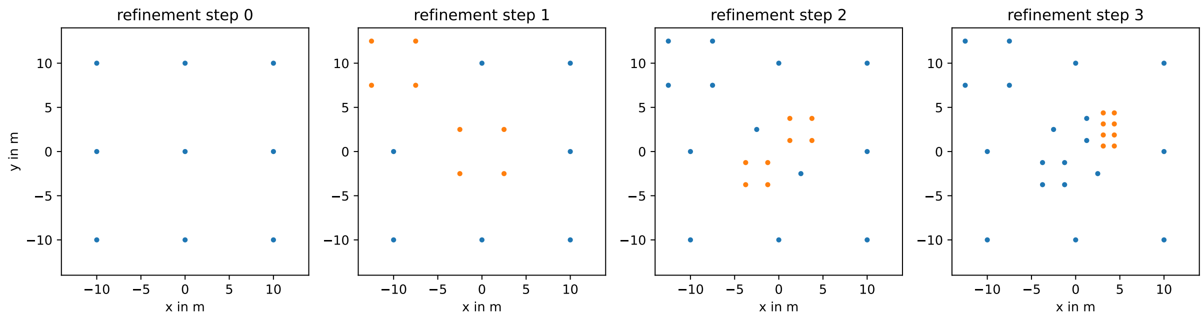

Figure 5: Successive grid refinement. In four steps certain areas of the grid are refined. New points are highlighted in orange.

DATA ANALYSIS

In order to test the methods and implementations, a test case was simulated using the `python`-package `acoular` [1]. The test case included three sources rotating with constant speed. Since positions and pressure levels are known, the results can be checked for accuracy. Figure 6 depicts three beamforming results using different point spacing of the grid. The accuracy of source positions increases with resolution.

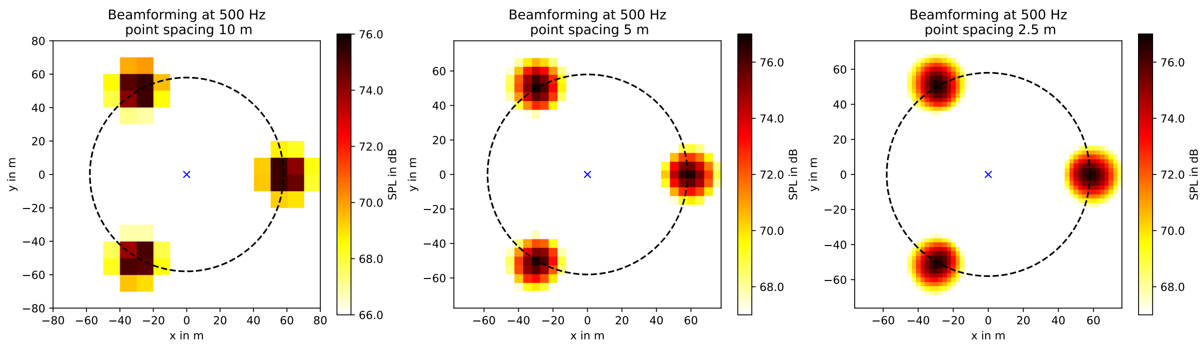

Figure 6: Beamforming results at 500 Hz *of a simulated case with three rotating sources analysed with different grid resolutions.*

During the measurement in 2024, carried out at the DLR research wind farm WiValdi, two wind turbines were active. The analysis focusses on the one closer to the microphone array. 101 microphones were positioned at distance of around 100 m from the base of the wind turbine over an area of 6 m by 12 m. Details can be found in [9]. The setup is shown in Figure 7.

During the measurement, 29 recordings were made, each lasting 60 s, for different configurations of the wind turbines.

The orientation of the wind turbine is dependent on the direction of the wind. The rotor plane can turn around the vertical y-axis (yaw angle) and tilt around the lateral x-axis (pitch angle).

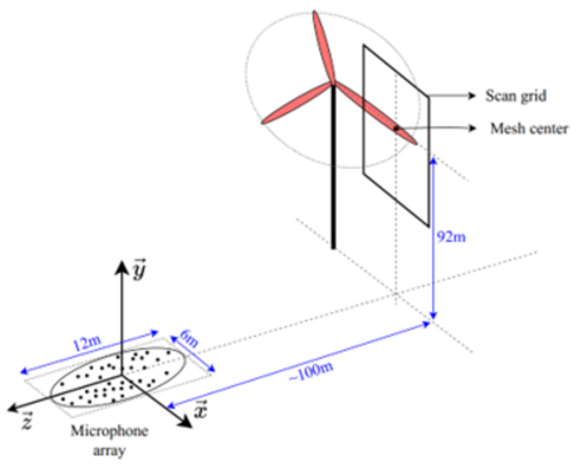

Figure 7: Measurement setup. The microphone array is located approximatly 100 m *from the wind turbine OPUS 2.*

The sensors of the wind turbine have a tolerance, which leads to measurement uncertainties when determining the yaw angle. Both angles have to be considered in the analysis of the data. A sketch is shown in Figure 8. Due to the wind direction, the wind turbine was viewed from behind during the measurements. For the analysis, this implies the anti-clockwise rotation of the wind turbine in the image plane.

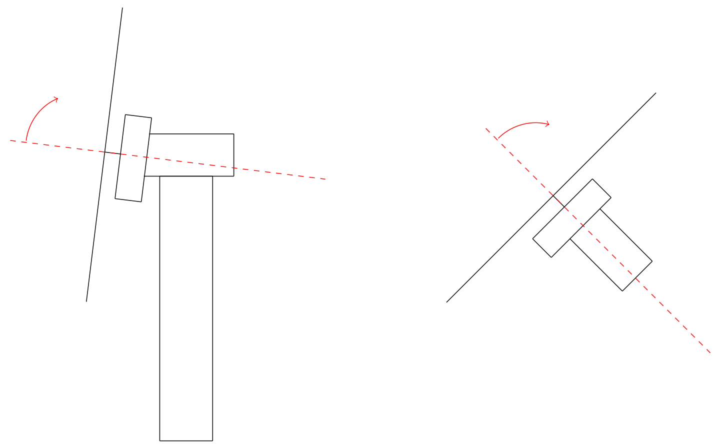

Figure 8: The pitch angle, shown on the left, and the yaw angle, shown on the right.

Prior to the beamforming analysis the raw data have been checked for intensity and validity. Figure 9 shows several spectra from selected microphones averaged over time and the spectrogram of one microphone over 60 s. The microphones have similar power spectra and the signal is also very regular over time. Both plots show a peak at approximately 150 Hz. This frequency should be taken into account in the subsequent analysis.

A low-frequency sound can be heard in the recordings. The beamforming result for the 160 Hz third octave band, which contains this frequency, is shown in Figure 10. On the left-hand side, a static grid is used for the beamforming algorithm. A large source region can be seen

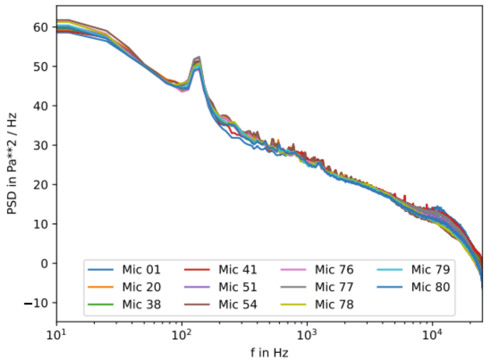

Power spectral density of selected microphones across the frequency range.

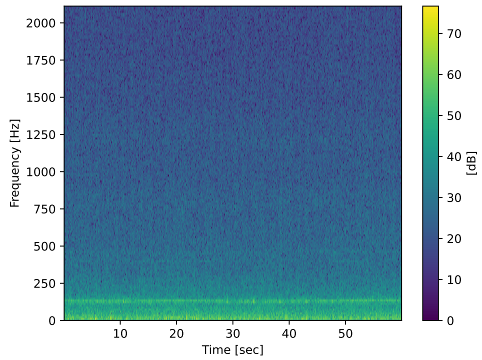

Spectrogram of a microphone during a 60 s *recording.*

Figure 9: Elevated levels at 150 Hz *can be seen both in the microphone spectra and in the spectrogram.*

above the position of the hub. In the rotating grid on the right-hand side of the Figure, this source region is rotated into a ring. The characteristics of the microphone array do not allow for greater accuracy in source localisation at this frequency. The identified sources are likely to be sources caused by the generator, which are not mapped onto the hub due to inaccuracies in the assumed geometry.

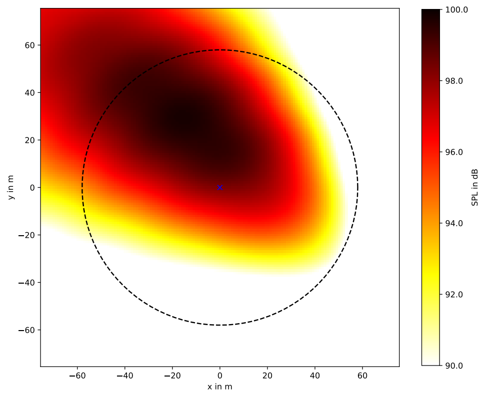

Beamforming sourcemap at 160 Hz *when using a static grid with a point spacing of* 1 m.

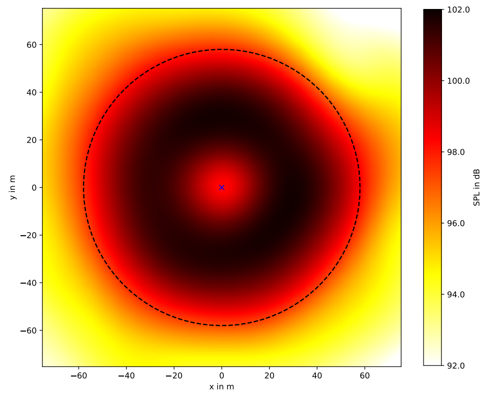

Beamforming sourcemap at 160 Hz *when using a rotating grid with a point spacing of* 0.5 m.

Figure 10: Source maps of the beamforming results of record 14 at the 160 Hz *third octave band.*

After examining the raw data and calculating initial beamforming results in the static system to provide a rough assessment of the data sets, the algorithms presented are applied to a number of selected recordings. Although the rotation of wind turbines is a relatively slow movement, the length of the rotor blades results in high speeds at the blade tips. During the recordings analyzed, the wind turbine rotates at a rate of one revolution in 4.5 s, which corresponds to a speed at the blade tips of approximately 808 m/s. The movement of the rotor blades creates aeroacoustic excitation causing pressure fluctuations with a strong directional characteristic, making the downward movement of a blade appears loudest [6]. The sources generated at the hub do not change position and stay in the same position. This makes them appear more prominent. Figure 11 gives an overview over all three methods for results within one octave. From left to right the sourcemaps of the beamforming, traditional CLEANT and CLEANT using successive grid refinement are shown. The first two methods shown in the first two columns use an equidistant grid with a distance of 2.5 m between points. The initial distance between points of the grid of the CLEANT with grid refinement is 4 m. However, as the frequency increases the resolution improves and the source regions can be reconstructed with greater precision in all methods. Visually, there is hardly any difference between the last two algorithms at this point already. Even with higher resolutions, the results of both CLEANT methods are equivalent. Since using the successive grid refinement method reduces computation time by a factor of 50, in further calculations only this method is used.

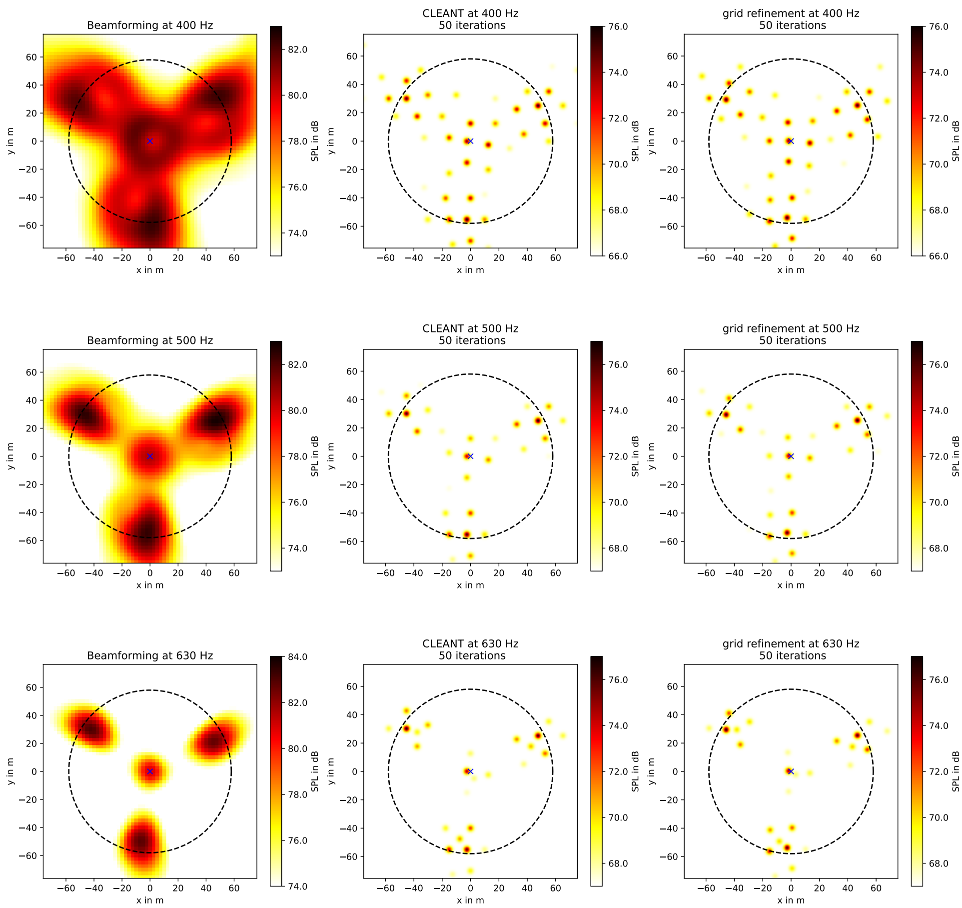

Figure 11: Sourcemaps of record 14 with three different methods. The frequencies shown correspond to three third-octave bands.

In the previous results using the CLEANT algorithms a scaling factor of $\gamma = 0.5$ was used.

In order to resolve distributed sources along the blade edges a smaller scaling factor should be considered. The results with two different values for γ are shown in Figure 12. When choosing a smaller γ the number of iterations should be increased as there is less energy transferred from *Dirty Map* to *Clean Map* in each iteration.

The maps show that sources are located closer together when using a smaller value for γ.

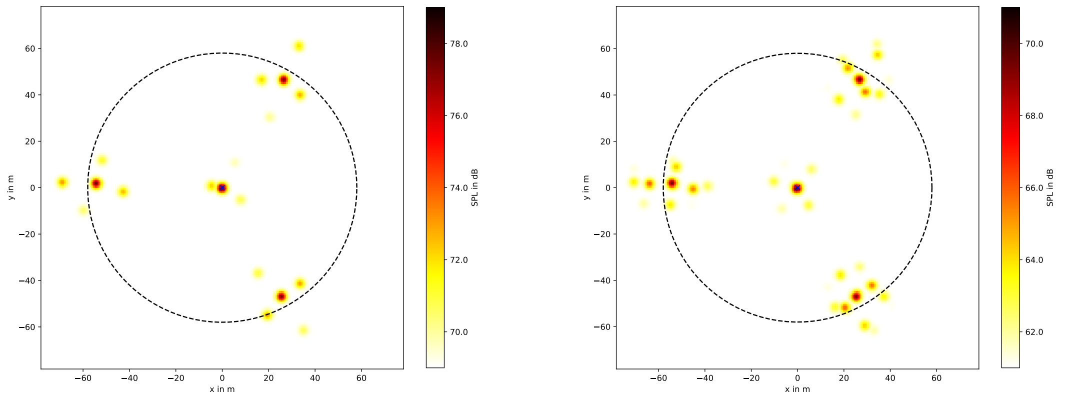

Clean Map of record 21 at 360 Hz *after 200 iterations with* $\gamma = 0.5$ *using successive grid refinement*

Clean Map of record 21 at 360 Hz *after 200 iterations with* $\gamma = 0.2$ *using successive grid refinement*

Figure 12: Different scaling factors when using a CLEANT algorithm represent distributed sources differently.

Sourcemaps shown in this paper all have a dynamic range of 10 dB. Due to the logarithmic scale, a larger range would make the differences of sound pressure levels in the final results less visible. In Figure 13 the loss of energy in the *Dirty Map* is shown as a function of the number of iterations. A possible stopping criterion could be the reduction of the total energy in the *Dirty Map* by 10 dB since a greater difference is not visible in the sourcemaps.

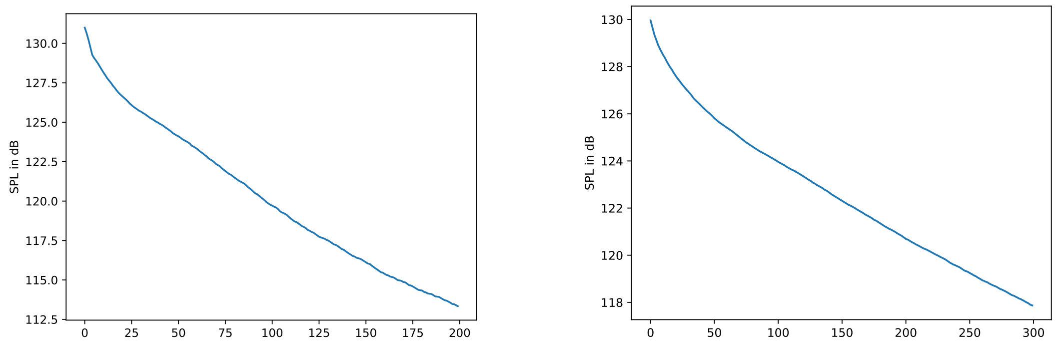

200 iterations with $\gamma = 0.5$

300 iterations with $\gamma = 0.2$

Figure 13: Total energy in Dirty Map using different values for γ *as a function of the number of iterations. In both cases, the energy decreases monotonically, but it decreases more rapidly when a higher scaling factor is used.*

In further calculations, the number of refinement steps using the refined grid is increased and the value of γ is even lower, both in order to achieve higher precision in the final results. Both variables allow for a better spatial resolution. For the sourcemaps in Figure 14 the number of refinement steps was increased, the shortest distance between points in the final grid is 0.25 m. Furthermore, on the right hand side, the scaling factor is reduced to 0.1. As a result, the distributed sources are more accuratly represented.

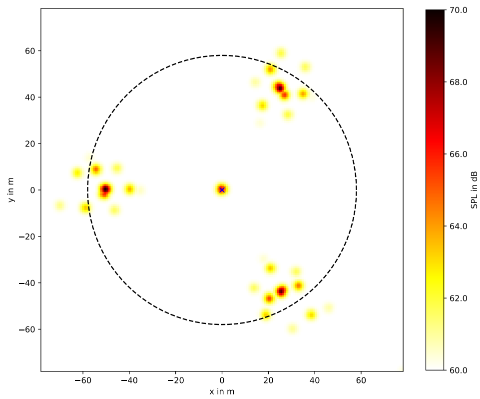

Clean Map of record 29 at 360 Hz *after 300 iterations with* $\gamma = 0.2$ *using successive grid refinement with four refinement steps*

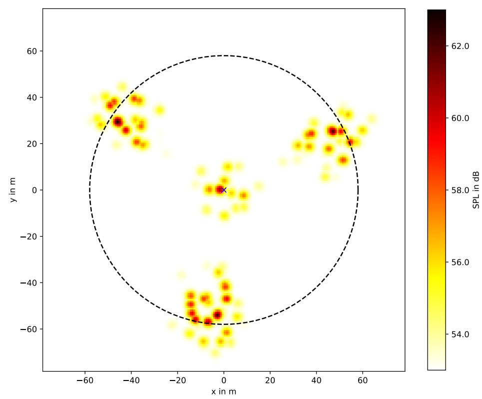

Clean Map of record 14 at 360 Hz *after 200 iterations with* $\gamma = 0.1$ *using successive grid refinement with four refinement steps*

Figure 14: Reducing the scaling factor γ *and increasing the number of refinement steps allows for a higher spatial resolution of the results.*

3 CONCLUSIONS

The data obtained from the DLR measurement at the wind farm have been successfully analyzed using three different methods for sound source localisation. Beamforming is the base of all used methods but can be improved by the CLEANT algorithm and by using successive grid refinement.

Traditional beamforming delivers reliable results with low computational effort, but its spatial resolution is limited by the beamwidth of the microphone array. The runtime depends primarily on the number of points used to scan the rotor plane. The CLEANT algorithm performs beamforming in each iteration and then models the signal of the detected maximum source across the microphone signals. To estimate the runtime of the algorithm, given the same point spacing in the grid to be analyzed, the runtime of the beamforming algorithm can be multiplied by the number of iterations. With equivalent results, the computation time was significantly reduced by using successive grid refinement. The number of points to be calculated is increased by only a fixed number of 40 points at specific locations instead of using a small distance between points on the whole grid. The CLEANT algorithm allows for a cleaner mapping of the sound sources. This advantage is also retained in the refined grid method.

4 ACKNOWLEDGEMENTS

This work was funded by the German Federal Ministry for Economic Affairs and Climate Action in the framework of the research project Deutsche Forschungsplattform für Windenergie DFWind under grant number FKZ 0325936 and by the Deutsche Forschungsgemeinschaft (DFG, German Research Foundation) in the framework of the projects LION and LION-2 under grant number 422372636. All pictures are licensed by DLR (CC BY-NC-ND 3.0).

REFERENCES

[1] "Acoular." `https://www.acoular.org/`. Accessed: 15.12.2025.

[2] J. Billingsley and R. Kinns. "The Acoustic Telescope." *J. Sound Vib.*, 48, 485–510, 1976. doi:10.1016/0022-460X(76)90552-6.

[3] R. Cousson, Q. Leclère, M.-A. Pallas, and M. Berengier. "A time domain clean approach for the identification of acoustic moving sources." *Journal of Sound and Vibration*, 443, 2019. doi:10.1016/j.jsv.2018.11.026.

[4] G. A. C. (DLR). "Homepage of the DLR research wind farm WiValdi.", 2025. `https://windenergy-researchfarm.com` [Accessed: 29.03.2026].

[5] E. Fehratovic. *An investigation of algorithms for sound source localization of complex moving objects*. Master's thesis, Chalmers University of Technology, 2022.

[6] S. Oerlemans. *Detection of aeroacoustic sound sources on aircraft and wind turbines*. Phd thesis, University of Twente, Enschede, 2009. URL `http://doc.utwente.nl/67363/1/thesis_S_Oerlemans.pdf`.

[7] T. Schumacher and H. Siller. "Beschleunigte Lokalisierung von bewegten Schallquellen mit CLEANT und einem Mehrgitterverfahren." In *Fortschritte der Akustik - DAGA 2024*, Fortschritte der Akustik - DAGA 2024. Deutsche Gesellschaft für Akustik e.V., 2024. doi:10.5281/zenodo.14925217. URL `https://elib.dlr.de/203703/`, diese Arbeit wurde im Rahmen des internationalen Forschungsprojekts Localization and Identification Of moving Noise sources (LION) von der Deutschen Forschungsgemeinschaft (DFG) gefördert.

[8] P. Sijtsma. "Experimental techniques for identification and characterisation of noise sources." Technical Report NLR-TP-2004-165, 2004.

[9] H. Siller. "Acoustic Source Localization on Wind Turbines." In *DAGA*. Deutsche Gesellschaft für Akustik, Dresden, 2026.